Biophysical Reviews and Letters
Vol. 8, Nos. 1 & 2 (2013) 21–32

DOI: 10.1142/S1793048012500099

World Scientific
www.worldscientific.com

DERIVING AN ELECTRIC CIRCUIT EQUIVALENT MODEL OF CELL MEMBRANE PORES IN ELECTROPORATION

B. I. MORSHED*,§, M. SHAMS† and T. MUSSIVAND‡

*Department of Electrical and Computer Engineering
The University of Memphis, TN 38152, USA

†Department of Electronics, Carleton University
Ottawa, ON K1S 5B6, Canada

‡Medical Devices Innovation Institute
The University of Ottawa, Ottawa, ON K1Y 4W7, Canada
§bmorshed@memphis.edu

Received 17 June 2012
Revised 27 November 2012
Accepted 28 November 2012
Published 10 January 2013

Electroporation is the formation of reversible pores in cell membranes under a brief pulse of high electric field. Dynamics of pore formation during electroporation suggests that the transmembrane potential would settle approximately at the threshold transmembrane potential and the transmembrane resistance would decrease significantly from the state of relaxation. The current electric circuit equivalent models for electroporation containing time-invariant, static and passive components are unable to capture the pore dynamics. A biophysically-inspired electric circuit equivalent model containing dynamic components for membrane pores has been derived using biological parameters. The model contains a voltage-controlled resistor driven by a two-stage cascaded integrator that is activated through a voltage-gated switch. Simulation results with the derived model showed higher accuracy compared to a commonly used model, where the transmembrane resistance decreased million-fold at the onset of electroporation and the transmembrane potential settled at 99.5% of the critical transmembrane potential, thus enabling improved dynamic behavior modeling ability of the pores in electroporation. The derived model allows fast and reliable analysis of this biophysical phenomenon and potentially aids in optimization of various parameters involved in electroporation.

Keywords: Electroporation; Electric circuit equivalent model; Transmembrane potential.

1. Introduction

When a biological cell is subjected to an electric pulse of intensity in the range of kilovolts-per-centimeter and duration in the range of microseconds-to-milliseconds, numerous hydrophilic pores are formed in the cell membrane and a temporary loss of the semi-permeability of the cell membrane occurs.[1–8] This phenomenon, called

electroporation (EP) or electropermeabilization, has many medical applications,[9] such as drug delivery,[10,11] gene therapy,[12,13] other macromolecules[14] and dye uptake,[15] and tumor and cancer treatment.[16] Nanosecond duration pulses can severely affect intracellular organelles, whereas effects of microsecond duration pulses are mostly observed in the cell membrane.[17,18] Effective modeling ability of EP is necessary to understand, predict and optimize various factors including excitation parameters such as magnitude, frequency, waveform shape and number of pulses,[19–22] cell size and shape,[23,24] cell orientation,[22] and the molecular update mechanism.[25]

Transmembrane potential, the potential developed across the cell membrane due to the applied electric field, is a crucial parameter of EP and dictates the onset of pore formation.[26] Experimental findings of the dynamics of EP have shown that when transmembrane potential reaches a critical threshold value, from 20 mV up to 1 V for various cell types,[5,27,28] numerous hydrophilic pores,[29] dependent on the magnitude of the applied electric field,[30] are formed in the cell membrane. These pores, primarily observed forming towards the electrodes,[27,31] expand in diameter with time if the electric field is sustained until an unstable pore diameter is reached (eg. 50 nm[32]). Consequently, the membrane conductivity increases, which counteracts the increment of transmembrane potential. This self-regulating feedback mechanism translates to the conductivity increase and settles such that the transmembrane potential stabilizes at the critical (threshold) transmembrane potential; an equilibrium condition[33] similar to a dynamic control system.[34] Current electric circuit equivalent modeling approaches are unable to capture the pore dynamics effectively,[35] even though some mathematical models produce representative waveforms.[19,33,36,37] Molecular dynamics approaches allowed clear understanding of biophysical phenomena occurring during pore formation.[25,38] This mismatch of electric circuit model is primarily due to the use of only time-invariant, static, passive components, such as fixed resistors, capacitors and potentials (Figs. 1(a) to 1(c)).[17,23,32] Transport lattice and meshed network models partially captured the dynamic behavior using transient pore density-dependent current source by incorporating the Neu–Krassowska asymptotic model of electroporation,[39–41] however the dynamic behavior of transmembrane potential and transient pore radius were not included. We investigated a new approach to develop a biophysically inspired electric circuit pore model that captures the dynamics of pore formation and expansion as well as dynamic transmembrane potential by incorporating dynamic, time-variant and active components to model the cell membrane pore (Fig. 1(d)).

2. Resistance of Membrane Pores

In this model, the hydrophilic pores formed at the onset of EP are approximated to be of cylindrical shape (Fig. 2), based on molecular dynamics simulations.[25,38] This is, however, a simplification of the known and complex structure of cell membranes with scope for refinement. The height of these cylindrical pores, d_m, is the thickness

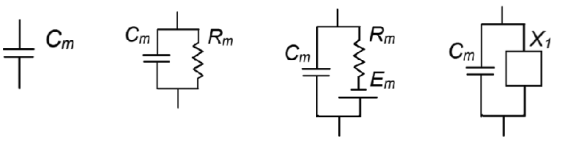

Fig. 1. **Electric circuit equivalent models.** (a–c) Electric circuit models for bilayer membrane of a cell in EP contain only fixed components of resistors (R_m), capacitors (C_m) and potentials (E_m). (d) The proposed model for bilayer cell membrane in EP that contains a dynamic pore element (X_1) in parallel to the capacitive element of the cell membrane (C_m).

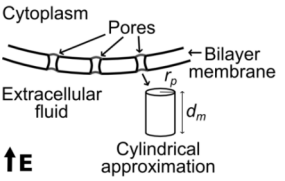

Fig. 2. **Cylindrical approximation for membrane pore resistance.** Cylindrical approximation of pores in a bilayer membrane of a cell in EP due to an applied electric field, E.

of the bilayer membrane of the cell. The radii of these pores, $r_p(t)$, are a function of time, t, and increase with time if excitation is sustained. These pores contain fluids infusing from the extracellular fluid (buffer medium) and the cytoplasm with resistivities of ρ_B and ρ_C, respectively. For physiological solutions, the values of these parameters are almost identical.[35,42] (In all subsequent expressions, ρ_B is used; however ρ_C can also be applied interchangeably.) One may calculate the transient value of a pore resistance, $R_p(t)$, by

$$R_p(t) = \frac{\rho_B d_m}{\pi r_p(t)^2}. \tag{1}$$

The transmembrane potential, V_{TM}, develops when an applied electric field, E, acts on a cell inside an extracellular fluidic environment. When V_{TM} reaches a critical value, many hydrophilic pores begin to form in the membrane. The number of hydrophilic pores on each half of the cell, $n_p(V_{TM})$, during EP is dependent on the applied amplitude and shape of the electric waveform,[30,38] and thus a function of the transmembrane potential, V_{TM}. For modeling purposes, all pores can be assumed to be formed at the same instant, and to expand at the same rate; thus all pores have the same size at any particular instant. In addition, all pores in one half of the membrane are in parallel. Hence, the total transient transmembrane resistance of one half of the cell, $R_{TM}(t)$, can be calculated as,

$$R_{TM}(t) = \frac{R_p(t)}{n_p(V_{TM})} = \frac{\rho_B d_m}{n_p(V_{TM})\pi r_p(t)^2} = \frac{K}{n_p(V_{TM}) r_p(t)^2} \tag{2}$$

where $K = \frac{\rho_B d_m}{\pi}$ is a proportionality constant. The number of pores, n_p, is a function of the transmembrane potential (V_{TM}), whose density can be expressed as

$N_0 e^{q(V_{TM}/V_{ep})^2}$, where N_0 is the equilibrium pore density when $V_{TM} = 0$, q is pore creation rate, and V_{ep} is the characteristic voltage of electroporation.[33] The rate coefficient of pore formation is also dependent on the pulse duration.[43] The pore expansion rate, $dr_p(t)/dt$, is determined by a set of ordinary differential equations, $U(r_p, V_{TM}, \sigma)$, where U is the advection velocity.[33] However, other models exist that differ from this model,[19] and a widely accepted model is a topic of future study. The pore sizes, $S_P(t)$, expand exponentially with the relationship of $S_P(t) = S_{P1} \exp(-t/\tau)$, where S_{P1} is the initial pore size and τ is the time constant.[44] Furthermore, it has been shown that the pore resealing rate is generally constant.[45] Hence, there is a linear relationship with pore diameter and elapsed time (i.e. $r_p(t) = K_2 t$). As a first order estimation, $n_p(V_{TM})$ is considered directly proportional to V_{TM} (i.e. $n_p(V_{TM}) = K_1 V_{TM}$) as well. Thus,

$$R_{TM}(t) = \frac{K}{K_1 V_{TM} K_2^2 t^2} = \frac{K_3}{V_{TM} t^2} \tag{3}$$

where $K_3 = \frac{K}{K_1 K_2^2}$ is another proportionality constant.

3. Deriving the Electric Circuit Pore Model

According to Eq. (3), the electric circuit pore model must consist of a voltage-controlled resistor, R_{TM}, which achieves the following relationship,

$$R_{TM} = \frac{K_4}{V_0} \tag{4}$$

where K_4 is the proportionality constant of the voltage-controlled resistor whose input voltage is V_0. By equating Eq. (4) with Eq. (3),

$$\frac{K_3}{V_{TM} t^2} = \frac{K_4}{V_0} \Rightarrow V_0 = \frac{K_4 V_{TM} t^2}{K_3} = K_5 V_{TM} t^2 \tag{5}$$

where $K_5 = \frac{K_4}{K_3}$ is a proportionality constant. Equation (5) can be realized by a two-stage cascaded integrator with an input voltage of V_{TM} (Fig. 3). The corresponding expression is,

$$V_0 = \frac{V_{TM}}{R_1 C_1 R_2 C_2} \int_0^t \int_0^t dt, dt = \frac{V_{TM} t^2}{2 R_1 C_1 R_2 C_2}. \tag{6}$$

Here, R_1, R_2, C_1, C_2 are the resistances and capacitances in the two-stage cascaded integrator. Equating Eq. (6) with Eq. (5), we get

$$K_5 = \frac{1}{2 R_1 R_2 C_1 C_2}. \tag{7}$$

The schematic diagram of the electric circuit pore model of membrane pores in EP is shown in Fig. 3 that includes the voltage controlled resistor (U_1) driven by the two-stage cascaded integrators (U_2 and U_3). The dynamic output resistance, R_{TM}, of U_1 is governed by Eq. (4), where V_0 is the output of the second integrator, U_2. The input of the first integrator, U_3, is the transmembrane potential, VTM

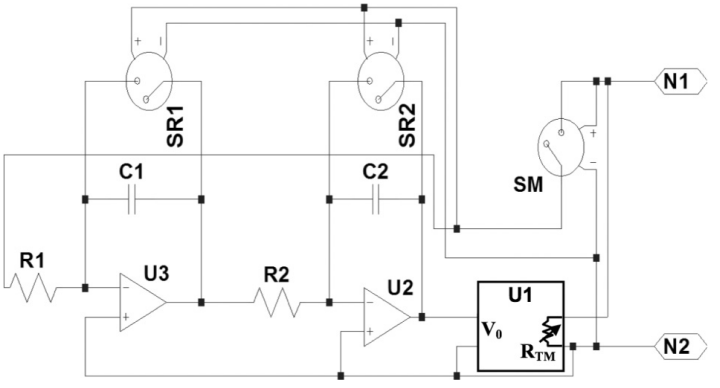

Fig. 3. **Derived electric circuit equivalent model.** The schematic diagram of the derived electric circuit equivalent model of the dynamic pore element, X_1.

(the voltage difference between nodes N_1 and N_2), connected through a voltage-controlled switch (SM). The pore opening and resealing phenomenon is modeled through this switch, SM, that closes as VTM becomes larger than the critical transmembrane potential, and opens as VTM becomes less than (arbitrarily chosen) 99% of the critical transmembrane potential.

Two voltage-controlled switches (SR_1 and SR_2) are included in the model that allows resetting of the integrators representing the completion of the resealing process. If the input voltage of U_3 decreases beyond a certain value, SR_1 and SR_2 closes to trigger complete discharge the capacitors, C_1 and C_2, of the integrators, U_3 and U_2, through the internal resistances of SR_1 and SR_2, respectively. This enables a practical time-bounded reset of the system, representing return to the original stable state of the cell membrane after EP.

4. Simulation Results

In this section, a commonly used model and the derived model were simulated and compared. In the commonly used electric circuit model, the cell membrane was represented by a parallel combination of a resistive element, RM, and a capacitive element, CM, whereas the cytoplasm resistance was represented by RC (Fig. 4(a)). The complete circuit diagram for simulation included a power supply, modeled with a pulse voltage source, V_1, with an internal resistance, RSS, and a microchannel with buffer fluid, modeled with a parallel combination of a capacitive element, CB, representing the capacitance across the opposite electrodes; and two resistive elements: RSB was the buffer resistance in series with the cell, and RPB was the buffer resistance in parallel of the cell. Using circuit theory, the circuit given in Fig. 4(a) was reduced to Fig. 4(b). In the proposed modeling approach, the derived model, X_1, replaced 2RM, as shown in Fig. 4(c). The values of the parameters and components were calculated from material properties and microchannel dimensions,

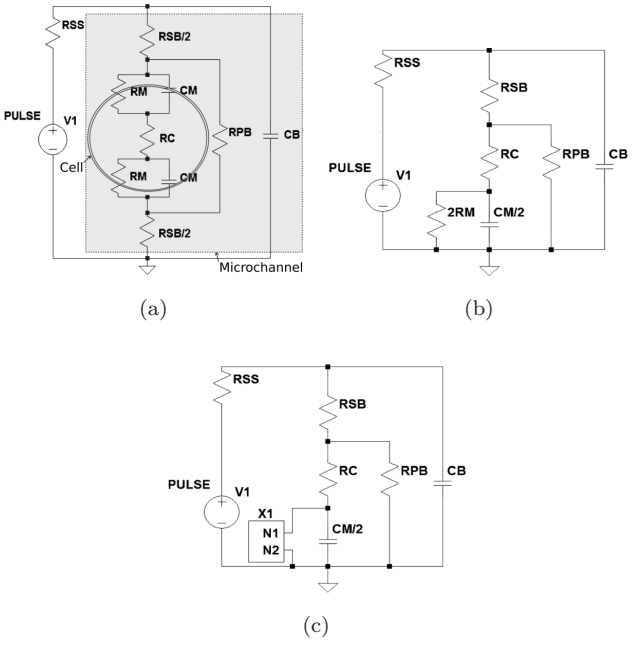

Fig. 4. **The complete circuit diagram for simulation of a cell inside a microchannel.** (a) An electric circuit model[17,23,32] of a cell inside a microchannel where the cell membrane is represented by a parallel combination of RM and CM. (b) Reduced element electric circuit model of (a) using circuit theory, where the combined cell membrane is represented by 2RM and CM/2. (c) The developed electric circuit equivalent model with the dynamic pore element, X_1, that replaces 2RM.

Table 1. Parameters related to the electric circuit equivalent model.

Parameter	Description	Value	Ref.
r_a	Radius of the cell	$5\,\mu$m	[32]
d_m	Thickness of cell membrane	5 nm	[35]
ρ_B	Resistivity of the buffer	3.3 Ω-m	[35, 42]
ρ_c	Resistivity of the cytoplasm	3.3 Ω-m	[35, 42]
ρ_m	Resistivity of the membrane	2 MΩ-m	[35]
ε_0	Dielectric permittivity of the vacuum	8.85×10^{-12} F/m	[35]
ε_m	Relative permittivity of the membrane	5	[35]
ε_B	Relative permittivity of the buffer fluid	80	[23, 35]
ε_C	Relative permittivity of the cytoplasm	80	[23, 35]
r_p	Radius of a pore	< 50 nm	[32]

and using reasonable arbitrary values for others as shown in Tables 1 and 2. The following rationales (Δ) have been adopted:

(1) Both stages of the cascaded integrators were considered to be identical (i.e. $R_1 = R_2$, $C_1 = C_2$).
(2) Arbitrarily, the values of K_1 and K_2 were considered to be 1000 (i.e. the number of pores to be a thousand fold of the transmembrane potential) and unity,

Table 2. Values of various components used in the simulation of the electric circuit equivalent models.

Component	Description	Value	Source
R_1	Resistive component of the first integrator	1 MΩ	A(Δ1)
R_2	Resistive component of the second integrator	1 MΩ	A(Δ1)
C_1	Capacitive component of the first integrator	1 μF	A(Δ1)
C_2	Capacitive component of the second integrator	1 μF	A(Δ1)
RC	Cytoplasm resistance	0.4 MΩ	C(Δ3)
RM	Transmembrane resistance (stable state)	0.1 GΩ	C(Δ3)
CM	Transmembrane capacitance	0.7 pF	C(Δ3)
RSB	Series resistance of the buffer fluid	8.25 KΩ	C(Δ4)
RPB	Parallel resistance of the buffer fluid	8.5 KΩ	C(Δ4)
CB	Microchannel capacitance	0.1416 pF	C(Δ4)
V_1	Pulse voltage source	10 V	A
RSS	Internal resistance of power supply	100 Ω	A
K	Relates R_{TM} with n_p and r_p	5.25×10^{-9}	C(E2)
K_1	Relates n_p with V_{TM}	1000	A(Δ2)
K_2	Relates r_p with t	1	A(Δ2)
K_3	Relates R_{TM} with V_{TM} and t	5.25×10^{-12}	C(E3)
K_4	Relates R_{TM} with V_0	2.6×10^{-12}	C(E5)
K_5	Relates V_0 with V_{TM} and t	0.5	C(E7)
$SM_{ON(V)}$	Critical transmembrane potential	1 V	Refs. 27 and 46
$SM_{ON(R)}$	ON resistance	0.1 Ω	A
$SM_{OFF(V)}$	Transmembrane potential for resealing	0.99 V	A
$SM_{OFF(R)}$	OFF resistance	10^{20}Ω	A
$SR_{ON(V)}$	Trigger reset of integrators	0.05 V	A
$SR_{ON(R)}$	ON resistance	0.1 Ω	A
$SR_{OFF(V)}$	Reset of integrators complete	0.1 V	A
$SR_{OFF(R)}$	OFF resistance	10^{20}Ω	A

Legends: *A-Arbitrary, C-Computed, E-Expression, R-Reference, Δ-Rationale.*

respectively. The actual values can be derived from experimental results for any specific cell types.

(3) RC, RM and CM representing the cell were calculated with the approximation of cell being represented by a cylinder whose base area and height were equal to the cross-sectional area and diameter, respectively, of the spherical cell.

(4) RSB, RPB and CB were calculated with an arbitrary microchannel having dimensions of $4 \times 10^{-9}\,\mathrm{m}^2$ cross-sectional area and 20 μm length.

Simulations were performed using a SPICE simulator (LTspice IV, Linear Technology, CA, USA). Here, simulation results to validate and differentiate the derived model with the commonly used model[23,32,35,42] are presented (Fig. 5). The voltages are normalized with respect to (w.r.t.) the critical transmembrane potential (CTMP) and the resistance is plotted using an arbitrary unit. As observed in Fig. 5(a), the transmembrane potential in the current model reached a steady state value determined by the values of the R-C components of the circuit, and is not influenced by EP dynamics (i.e. pore formation) or CTMP. For example, the resulted transmembrane potential with an applied voltage of 10 V is 4.114 V whereas

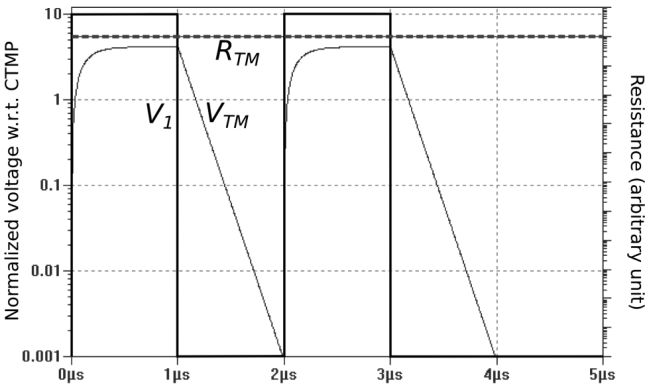

(a)

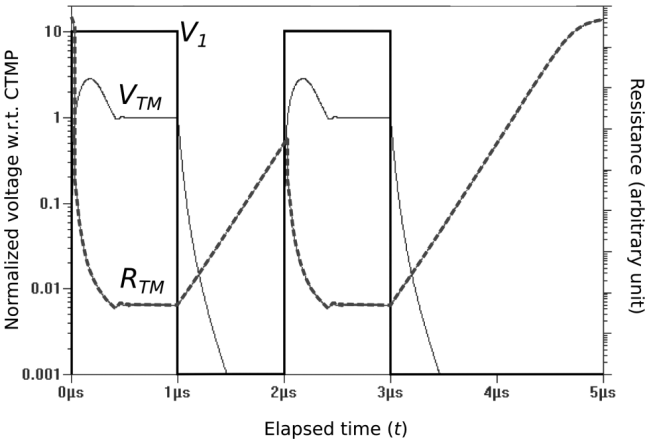

(b)

Fig. 5. **Comparison of simulation results.** Electric circuit simulation results of a cell exposed to 2 electric pulses of 1 μs duration using two electric circuit models: (a) a commonly used model, and (b) the derived model. Here, the applied voltage, V_1, and the transmembrane potential, V_{TM}, are normalized with respect to (w.r.t.) the critical transmembrane potential (CTMP), and the transmembrane resistance, R_{TM}, is plotted against an arbitrary unit using a log scale.

the maximum value of CTMP is reported to be 1 V.[27,46] In addition, the resistance of the cell membrane is constant throughout the simulation, which contradicts the expectation predicted from pore dynamics as discussed in Sec. 1.

Simulation results with the derived model (Fig. 5(b)), however, produced results that are in agreement with EP dynamics. When the pulse voltage is applied, the transmembrane potential increases. As the transmembrane potential crosses the critical value of 1 w.r.t. CTMP, pores are expected to form introducing new resistive paths, which is reflected (via SM) in the decrease of the transmembrane resistance. As pores expand, the resistance of these paths drops, resulting in the reduction

of the transmembrane resistance with time. This reduction of the transmembrane resistance reduces transmembrane potential, and in turn, contributes to stabilizing the transmembrane potential close to the critical transmembrane potential. Simulation results showed that, for any applied voltage that creates a transmembrane potential beyond CTMP, the transmembrane potential settles to a value near the critical transmembrane potential. For instance, with an applied voltage of 10 V, the transmembrane potential settles at 0.995 V for a transmembrane potential of 1 V,[27,46] and the steady-state value of transmembrane resistance decreases million-fold. The results from the proposed model are comparable to numerical models that well-correspond to EP dynamics.[33]

5. Conclusion

This paper provides the derivation of a new, biophysically inspired electric circuit equivalent model for membrane pores in EP that captures the dynamic, time-variant pore behavior. The derived model is proposed to replace the fixed resistance model that is used in conventional electric circuit modeling approaches. The simulation results clearly demonstrate the ability of the derived model to represent pore formation dynamics effectively during EP. Study of the pore resealing process indicates long-lived pores after withdrawal of electric pulse, on the order of 0.1 to 1 s^{-1}. This can be possibly achieved by analyzing the transient discharge of integrators with potential additional components. Thus, there is scope to improve the model to incorporate the dynamics of pore resealing process. Furthermore, meshed or lattice transport approaches to determine spatially distributed parameters are potential future research directions.

The model provides a biophysically motivated approach for modeling of biological elements. The model could be an effective tool to analyze various biological parameters related to EP including cell size, membrane thickness, pulse amplitude, wave-shape, repetition, and frequency, as well as microchannel and buffer related parameters towards optimized application of EP. Analysis of our previously reported experimental data[47] is currently undergoing. Furthermore, the derived model is fast, flexible, adjustable and expandable to incorporate a variety of other biophysical attributes including internal organelles, and the ability to model electrical lysis, which are some future research directions.

Acknowledgement

The authors would like to thank the anonymous reviewers and editors for their valuable comments, suggestions and insights to improve the quality of the paper.

References

1. K. Kinosita and T. Y. Tsong, Formation and resealing of pores of controlled sizes in human erythrocyte membrane, *Nature* **268**, 438–441 (1977).

2. R. Benz, F. Beckers and U. Zimmermann, Reversible electrical breakdown of lipid bilayer membranes: A charge-pulse relaxation study, *J Membrane Biol* **48**, 181–204 (1979).
3. J. C. Weaver, G. I. Harrison, J. G. Bliss, J. R. Mourant and K. T. Powell, Electroporation: High frequency of occurrence of a transient high-permeability state in erythrocytes and intact yeast, *FEBS Letters* **229**(1), 30–34 (1988).
4. J. C. Weaver, Molecular basis for cell membrane electroporation, *Ann NY Acad Sci* **720**, 141–152 (1994).
5. E. Neumann, A. E. Sowers and C. A. Jordan, *Electroporation and Electrofusion in Cell Biology* (Plenum Press, NY, USA, 1989).
6. K. J. Muller, V. L. Sukhorukov and U. Zimmermann, Reversible electropermeabilization of mammalian cells by high-intensity, ultra-short pulses of sub-microsecond duration, *J Membrane Biol* **184**(2), 161–170 (2001).
7. A. J. Sale and W. A. Hamilton, Effects of high electric fields on microorganisms I: Killing of bacteria and yeasts, *Biochimica et Biophysica Acta* **184**(3), 781–788 (1967).
8. J. C. Weaver, Electroporation of cells and tissues, *IEEE Trans Plasma Science* **28**(1), 24–33 (2000).
9. S. B. Dev, D. Rabussay, G. Widera and G. A. Hofmann, Medical applications of electroporation, *IEEE Trans Plasma Science* **28**(1), 206–223 (2000).
10. P. J. Canatella, M. M. Black, C. McKenna, J. K. Karr, J. A. Petros and M. R. Prausnitz, Electroporation of prostate cancer cells for drug delivery, *IEEE IEMBS* **1999**, 802124 (1999).
11. F. Behar-Cohen, Electroporation for ocular drug delivery, *Acta Ophthalmologica* **90**, s249 (2012).
12. S. Van Meirvenne, L. Straetman, C. Heirman *et al.*, Efficient genetic modification of murine dendritic cells by electroporation with mRNA, *Cancer Gene Ther* **9**, 787–797 (2002).
13. E. Neumann, M. Schaefer-Ridder, Y. Wang and P. H. Hofschneider, Gene transfer into mouse lyoma cells by electroporation in high electric fields, *EMBO J* **1**(7), 841–845 (1982).
14. S. I. Sukharev, V. A. Klenchin, S. M. Serov, L. V. Chernomordik and Y. Chizmadzhev, Electroporation and electrophoretic DNA transfer into cells. The effect of DNA interaction with electropores, *Biophys J* **63**, 1320–1327 (1992).
15. J. Belehradek, S. Orlowski, L. H. Ramirez, G. Pron, B. Poddevin and L. M. Mir, Electropermeabilization of cells in tissues assessed by the qualitative and quantitative electroloading of bleomycin, *Biochim Biophys Acta* **1190**, 155–163 (1994).
16. K. H. Schoenbach, R. Nuccitelli and S. J. Beebe, ZAP: Extreme voltage could be a surprisingly delicate tool in the fight against cancer, *IEEE Spectrum* **43**(8), 22–26 (2006).
17. K. H. Schoenbach, Ultrashort electrical pulses open a new gateway into biological cells, *Proc IEEE* **92**(7), 1122–1137 (2004).
18. W. Frey, J. A. White, R. O. Price, P. F. Blackmore, R. P. Joshi, R. Nuccitelli, S. J. Beebe, K. H. Schoenbach and J. F. Kolb, Plasma membrane voltage changes during nanosecond pulsed electric field exposure, *Biophysical J* **90**, 3608–3615 (2006).
19. Q. Hu, R. P. Joshi and A. Beskok, Model study of electroporation effects on the dielectrophoretic response of spheroidal cells, *J. Applied Physics* **106**(2), 024701 (2009).
20. B. L. Ibey, D. G. Mixon, J. A. Payne, A. Bowman, K. Sickendick *et al.*, Plasma membrane permeabilization by trains of ultrashort electric pulses, *Bioelectrochemistry* **79**(114), 1 (2010).

21. D. Miklavcic and L. Towhidi, Numerical study of the electroporation pulse shape effect on molecular uptake of biological cells, *Radiol Oncol* **44**, 34–41 (2010).
22. K. Maswiwat, D. Wachner and J. Gimsa, Effects of cell orientation and electric field frequency on the transmembrane potential induced in ellipsoidal cells, *Bioelectrochemistry* **74**, 130–141 (2008).
23. C. Yao, Y. Mi, C. Li, X. Hu, X. Chen and C. Sun, Study of transmembrane potentials on cellular inner and outer membrane — frequency response model and its filter characteristic simulation, *IEEE Trans Biomedical Engineering* **55**(7), 1792–1799 (2008).
24. A. Agarwal, I. Zudans, E. A. Weber, O. Orwar and S. G. Weber, Effect of cell size and shape on single-cell electroporation, *Anal Chem* **79**(10), 3589–3596 (2007).
25. Q. Hu, V. Shidhara, R. P. Joshi, J. F. Kolb and K. H. Schoenbach, Molecular dynamics analysis of high electric pulse effects on bilayer membranes containing DPPC and DPPS, *IEEE Trans Plasma Science* **34**(4), 1405–1411 (2006).
26. E. Neumann, Electric field-induced structural rearrangements in biomembranes, *Studia Biophysic* **130**(1–3), 139–143 (1989).
27. T. Kotnik, G. Pucihar and D. Miklavcic, Induced transmembrane voltage and its correlation with electroporation-mediated molecular transport, *J Membrane Biol* **236**, 3–13 (2010).
28. J. Teissie' and M. P. Rols, An experimental evaluation of the critical potential difference inducing cell membrane electropermeabilization, *Biophys J* **65**, 409–413 (1993).
29. Q. Hu and R. P. Joshi, Transmembrane voltage analysis in spheroidal cells in response to an intense ultrashort pulse, *Physical Review E* **79**, 011901-1-11 (2009).
30. P. Shil, S. Bidaye and P. B. Vidyasagar, Analysing the effects of surface distribution of pores in cell electroporation for a cell membrane containing cholesterol, *J of Physics D: Applied Physics* **41**, 055502-1-7 (2008).
31. M. Hibino, M. Shigemori, H. Itoh, K. Nagayama and K. Kinosita, Membrane conductance of an electroporated cell analyzed by submicrosecond imaging of transmembrane potential, *Biophysical J* **59**(1), 209–220 (1991).
32. R. P. Joshi and K. H. Schoenbach, Electroporation dynamics in biological cells subjected to ultrafast pulses: A numerical simulation study, *Physical Review E* **62**(1), 1025–1033 (2000).
33. W. Krassowska and P. D. Filev, Modeling electroporation in a single cell, *Biophysical J* **92**, 404–417 (2007).
34. G. F. Franklin, J. D. Powell and A. Emami-Naeini, *Feedback Control of Dynamic Systems* (Prentice Hall, NJ, USA, 2009).
35. G. Pucihar, D. Miklavcic and T. Kotnik, A time-dependent numerical model of transmembrane voltage inducement and electroporation of irregularly shaped cells, *IEEE Trans Biomedical Engineering* **56**(5), 1491–1501 (2009).
36. A. T. Esser, K. C. Smith, T. R. Gowrishankar, Z. Vasilkoski and J. C. Weaver, Mechanisms for the intracellular manipulation of organelles by conventional electroporation, *Biophysical J* **98**, 2506–2514 (2010).
37. K. A. DeBruin and W. Krassowska, Modeling electroporation in a single cell. I. Effects of field strength and rest potential, *Biophys J.* **77**(3), 1213–1224 (1999).
38. D. Moldovan, D. Pinisetty and R. V. Devireddy, Molecular dynamics simulation of pore growth in lipid bilayer membranes in the presence of edge-active agents, *Applied Physics Letters* **91**(20), 204104-1-3 (2007).
39. T. R. Gowrishankar and J. C. Weaver, An approach to electrical modeling of single and multiple cells, *Proc. Natl. Acad. Sci.* **100**, 3203–3208 (2003).
40. D. A. Stewart, T. R. Gowrishankar and J. C. Weaver, Transport lattice approach to describing cell electroporation: Use of a local asymptotic model, *IEEE Trans on Plasma Science* **32**(4), 1696–1708 (2004).

41. K. C. Smith and J. C. Weaver, Active mechanisms are needed to describe cell responses to submicrosecond, megavolt-per-meter pulses: Cell models for ultrashort pulses, *Biophysical J.* **95**(4), 1547–1563 (2008).
42. C. Yao, D. Mo, C. Li, C. Sun and Y. Mi, Study of transmembrane potentials of inner and outer membranes induced by pulsed-electric filed model and simulation, *IEEE Trans Plasma Science* **35**(5), 1541–1549 (2007).
43. E. Neumann, K. Toensing, S. Kakorin, P. Budde and J. Frey, Mechanism of electroporative dye uptake by mouse B cells, *Biophysical J* **74**, 98–108 (1998).
44. G. Pucihar, T. Koαtnik, D. Miklavc and J. Teissie, Kinetics of transmembrane and transport of small molecules into electropermeabilized cells, *Biophysical J* **95**, 2837–2848 (2008).
45. A. Agarwal, M. Wang, J. Olofsson, O. Orwar and S. G. Weber, Control of the release of freely diffusing molecules in single-cell electroporation, *Anal. Chem.* **81**, 8001–8008 (2009).
46. T. Y. Tsong, Electroporation of cell membranes, *Biophysics J* **60**, 297–306 (1991).
47. B. I. Morshed, M. Shams and T. Mussivand, Identifying severity of electroporation through quantitative image analysis, *Applied Physics Letters* **98**(14), 143704/1–3 (2011).